

Short Communication

Saccharin-assisted Galvanostatic Electrodeposition of Nanocrystalline FeCo Films on a Flexible Substrate

Setia Budi*, Rizqi Aulia Tawwabin, Ucu Cahyana, Afrizal, Maria Paristiowati

Department of Chemistry, Faculty of Mathematics and Sciences, Universitas Negeri Jakarta, Jl. Rawamangun Muka, Jakarta Timur 13220, Indonesia

*E-mail: setiabudi@unj.ac.id

Received: 1 March 2020 / *Accepted:* 27 April 2020 / *Published:* 10 June 2020

The electrodeposition of functional materials on a flexible substrate has become an interesting topic because of the current development of flexible devices, called flexible technology, for various electronic applications. This study investigated FeCo film electrodeposition on a flexible polyethylene coated with indium tin oxide using the galvanostatic technique. The obtained FeCo films have a very fine crystallite size with a uniform surface morphology that changed remarkably upon introduction of a saccharin additive and upon increasing the deposition temperature. The effect of the saccharin concentration and deposition temperature on the current efficiency and anomalous co-deposition of FeCo was discussed. In this work, electrodeposition from an electrolyte containing 1 g/L saccharin at a very high current efficiency and a low deposition temperature was successfully achieved. The obtained composition ratio indicated that saccharin could reduce the anomalous co-deposition of Fe and Co. This phenomenon was also observed at a high deposition temperature. These results convincingly show the high current efficiency and reduced anomalous characteristic of the saccharin-assisted electrodeposition of FeCo.

Keywords: High current efficiency electrodeposition, anomalous co-deposition, galvanostatic technique, saccharin additive, nanocrystalline FeCo

1. INTRODUCTION

Electrodeposition is a synthesis method used for the fabrication of oxides, metals and alloys using a relatively simple technology. Using the electrodeposition technique, the characteristics of the nanomaterials produced can be controlled by adjusting the reaction conditions, such as temperature, pH and potential or current density. Recently, electrodeposition has also been widely used as a bottom-up approach for the synthesis of nanostructured thin films. Among the materials that can be synthesised by electrodeposition is the FeCo binary alloy [1,2]. This alloy is of interest to many researchers because of its magnetic nature, which results in high magnetic saturation and permeability with a low coercivity

value [3,4]. These characteristics make FeCo an important material in various electronic devices, including as heads in magnetic recording devices and absorbers for electromagnetic interference.

In the last two decades, electrodeposition of a FeCo thin layer onto a variety of substrates was performed. Other than SiO₂ wafers [5] and indium tin oxide (ITO) conductive glass [6,7], the majority of the substrates used are metals such as platinum [1], titanium–gold [8], copper [1,9–12], brass [13,14] and titanium [15,16]. However, the development of near-future devices is considered to refer to flexible electronic devices, which require the availability of advanced materials that have not only high performance but also flexibility and a low weight-to-volume ratio [17–19]. Therefore, in this study, the electrodeposition of the FeCo thin layer was conducted on a flexible ITO-coated polyethylene (ITO-PET) substrate.

Among the important aspects that need to be considered in material synthesis using electrodeposition is current efficiency because it relates to the energy used and affects the cost of material fabrication. In general, the efficiency of the electrodeposition of FeCo is relatively low [13,20,21]. Efforts to increase the current efficiency have been made by adjusting the solution pH [22], voltage [20] or current strength, additive concentration and Fe²⁺ concentration [20,21]. The current efficiency increases as the pH of the solution increases with a pH of less than 3 [22]. The current efficiency is also known to increase only at high current densities or at very high voltage ranges (–0.9 to –1.2 V vs. SCE) [20]. Conversely, the adjustment of Fe²⁺ concentration does not produce the expected change because the current efficiency value is generally found to be independent of the metal ion content [13,20,21]. Another important aspect that must be considered in FeCo electrodeposition is the ability to control the chemical composition of the alloy because it is closely related to material properties, such as coercivity, magnetic saturation [6] and corrosion resistance [23]. In the case of Fe and Co electrodeposition, the chemical composition of the alloy is challenging; because both metals are iron-group metals, the electrodeposition of FeCo generally takes place anomalously [24], thus making it difficult to control the alloy composition. To control the chemical composition of alloys, various approaches have been conducted to overcome the characteristics of the anomalous co-deposition of FeCo by varying the mole ratio of FeCo [6,25], the deposition temperature [26,27] and the pH [6], indicating that whether the anomalous co-deposition characteristics can be reduced by eliminating them remains difficult. Another approach that has been widely investigated is introducing additives into the electrolyte. Among the additives showing many advantages in metal and alloy electrodeposition is saccharin. In addition to being environmentally friendly, saccharin is known for its ability to change the interface between the solution and electrode, which is expected to produce the desired effects on the electrodeposition processes of Fe-group metals and their deposit properties. Some previous works reported the use of saccharin to increase deposit ductility and surface brightness [28], control grain size and reduce surface roughness [28,29]. In addition, this additive also has the potential to increase the electrodeposition efficiency [29] and reduce anomalous electrodeposition characteristics [24,30]. The electrodeposition process is also known to be dependent on substrates that generally exhibit different charge transfer [31], active site characteristics and surface morphology that determine nucleation and deposit growth [32,33]. The effect of surface morphology, density and uniformity on electrodeposition was reported previously [33], indicating different deposition mechanisms occur on different substrates.

Based on the above background, in this study, the influence of saccharin and its concentration on increasing the current efficiency and reducing anomalous characteristics of FeCo electrodeposition on a flexible substrate, namely, ITO-PET, was investigated. FeCo electrodeposition was performed using a galvanostat. The effects of the deposition temperature on the current efficiency and anomalous co-deposition were also discussed.

2. EXPERIMENTAL DETAILS

The nanocrystalline FeCo films were electrodeposited from electrolyte solutions prepared with analytical-grade chemicals purchased from PT Merck Indonesia, and food-grade saccharin as the additive was supplied by PT Brataco Indonesia. The electrolyte composition contained 0.02 M FeSO₄·7H₂O, 0.08 M CoSO₄·7H₂O and 0.40 M H₃BO₃. The FeCo electrodeposition was carried out in a three-electrode cell with a platinum wire and Ag/AgCl as the counter electrode and reference electrode, respectively. For the working electrode, a polyethylene terephthalate (PET) substrate coated with a conductive layer of ITO (ITO-PET) was used with a deposition area of approximately 20 mm × 10 mm. The electrodeposition process was performed at a current density of 5 mA/cm², which was controlled using an Edaq EA163 potentiostat and e-corder 401. Electrodeposition was performed at three different temperatures between 5 °C and 50 °C. The concentration of saccharin in the electrolyte was varied from 0 to 5 g/L. The chemical content of the deposit was analysed using atomic adsorption spectroscopy (Shimadzu, AA700). The morphological analysis of the deposit was performed using a scanning electron microscope (Carl Zeiss, EVO MA10). Phase analysis and crystallisation measurements were conducted on an X-ray diffractometer (XRD) (PANanalytical, Empyrean) with Cu K α radiation ($\lambda = 1.5406 \text{ \AA}$) in the 2θ range of 30°–110° and a step size of 0.02°.

The influences of saccharin composition and deposition temperature on the current efficiency and anomalous co-deposition of FeCo were evaluated. The current efficiency (CE) of FeCo electrodeposition is the ratio of the actual deposit mass gained (w) to the theoretical Faraday's mass [34] calculated using equation (1)

$$CE = \frac{w}{\frac{Ew}{F} \times I \times t} \times 100 = \frac{wF}{I \times t} \sum \frac{c_a n_a}{M_a} \times 100 \quad (1)$$

where Ew is the equivalent weight of the deposit (g equiv⁻¹), I is the applied current (A), t is the electrodeposition time, F is Faraday's constant, c_a is the weight fraction of the metal in the deposit, n_a is the number electron to be transferred to deposit one atom of a metal, and M_a is the atomic mass of the metal. The anomalous co-deposition was examined in terms of the composition ratio of the wt% of the metal in the deposit to wt% of the metal in the electrolyte [35], as defined by equation (2):

$$\text{Composition ratio} = \frac{\text{wt\% of } m \text{ in the deposit}}{\text{wt\% of } m \text{ in the electrolyte}} \quad (2)$$

where m is the metal of Fe or Co.

3. RESULTS AND DISCUSSION

A FeCo thin film was successfully deposited on the ITO-PET substrate. The XRD diffraction patterns shown in Fig. 1 confirmed the formation of nanocrystalline FeCo through the appearance of

diffraction peaks at 2θ 45.16° (011), 66.10° (002) and 83.65° (112) corresponding to the reflection planes of (011), (002) and (112), respectively. This pattern agrees with PDF card number 00-037-0474. Crystallite size measurements conducted using the Scherrer equation showed very fine crystallites of the electrodeposited FeCo, with a size range of 16–49 nm (Fig. 2). The diffraction intensity and peak sharpness indicate the different crystallite sizes of each deposit. In addition, a high diffraction intensity from the sample electrodeposited in the presence of saccharin can be associated with the large grain that formed on the substrate, as shown in the micrograph obtained using SEM (Fig. 3). The micrograph shows that the film obtained from the electrolyte without saccharin was composed of relatively fine flower-like particles (Fig. 3a). The shape of the particles changed significantly to large starfish-like particles upon addition of 1 g/L saccharin, as shown in Fig. 3b. These results indicate the effect of saccharin on the changes in the orientation of FeCo deposition as a consequence of the adsorption of saccharin additive molecules on the active sites of the substrate where the deposit grows. Different deposit characteristics were also observed in the FeCo layer, which was deposited at a low deposition temperature of 5 °C (Fig. 3c). When the temperature was increased, the particles became larger than those of the sample electrodeposited at room temperature (Fig. 3d).

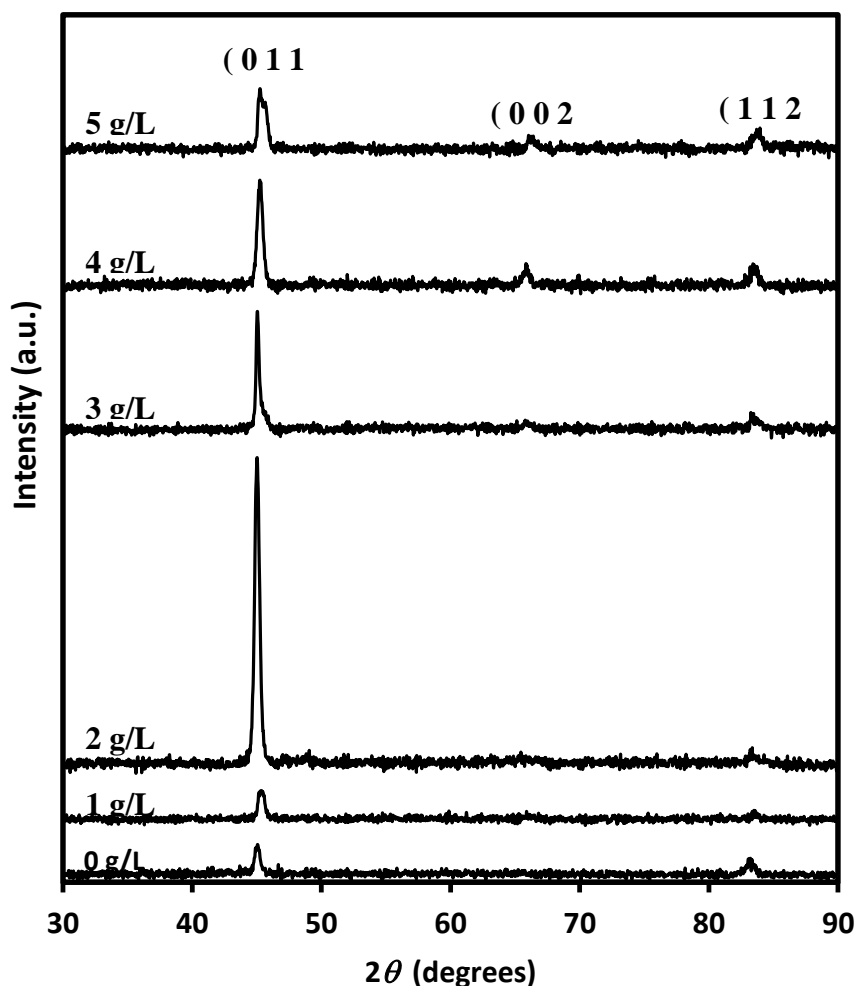


Figure 1. XRD patterns of the nanocrystalline FeCo films electrodeposited at room temperature from electrolytes containing 0 to 5 g/L saccharin.

Fig. 4a shows the weight percentage (wt%) of the Fe and Co contents of the film prepared at room temperature from the electrolyte with different concentrations of saccharin. The film synthesised from electrolytes without saccharin contained 52.7 wt% Co and 47.3 wt% Fe. This composition was different from the ratio of Co to Fe in the solution (4:1), indicating that Fe and Co co-deposition occurred anomalously. This anomalous co-deposition of Fe and Co can be ascribed to the hydrogen evolution that occurred along with the reduction of metals on the substrate. This evolution of hydrogen played a role in increasing the number of hydroxyl ions.

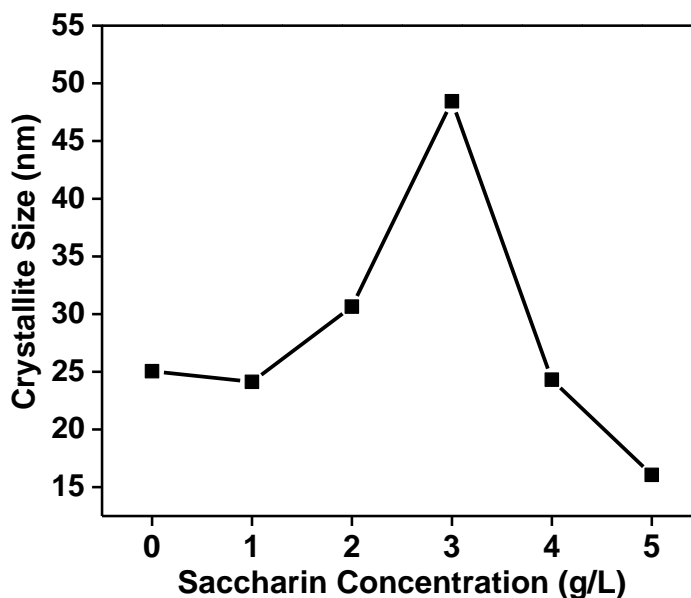
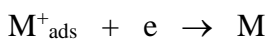


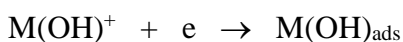
Figure 2. Crystallite size of the nanocrystalline FeCo films electrodeposited at room temperature from electrolytes containing different concentrations of saccharin from 0 to 5 g/L.

The increase in hydroxyl ions enhanced the formation of metal hydroxide ions, namely, $\text{Fe}(\text{OH})^+$ and $\text{Co}(\text{OH})^+$. Metal deposition occurs through the intermediate phase, which is the adsorption of ions in the form of both specific metal ions and complex ions as follows [36]:

metal ion adsorption:



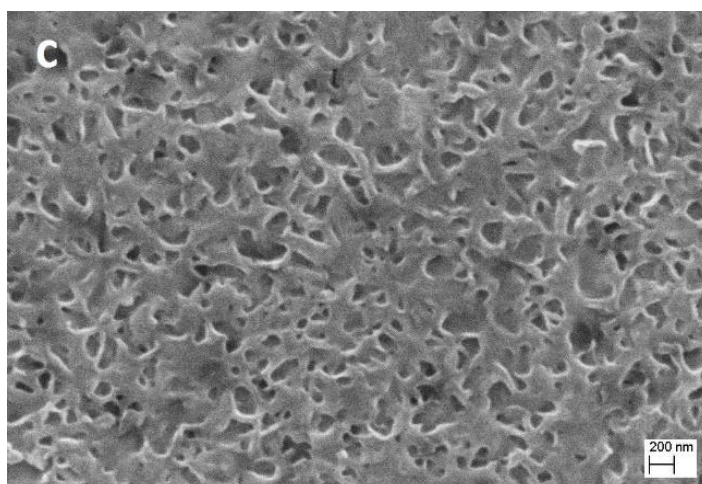
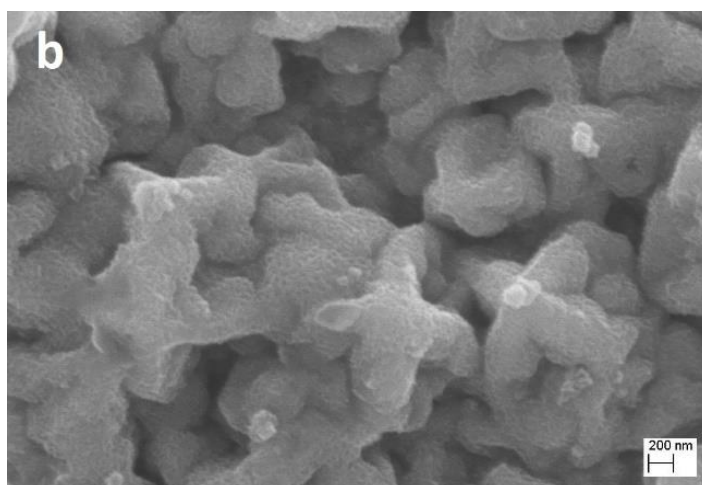
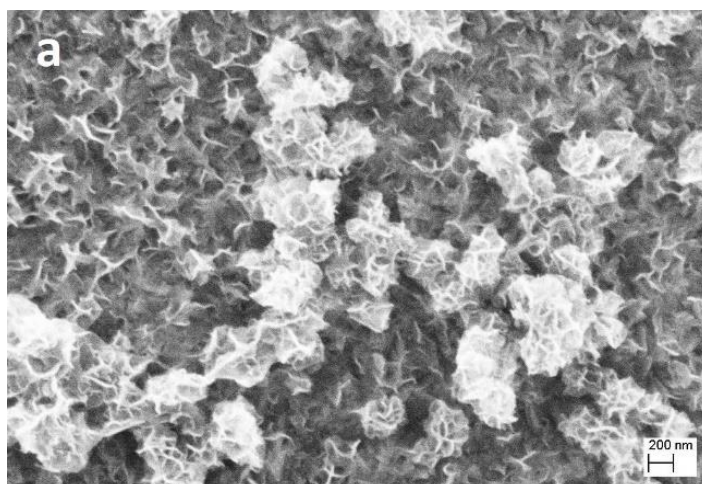
monohydroxide metal ion adsorption:



with M as the deposited metal.

The hydroxide ions compete to diffuse towards the active sites and are then adsorbed onto the substrate surface. $\text{Fe}(\text{OH})^+$ has a higher adsorbency preference than $\text{Co}(\text{OH})^+$. Therefore, indirectly, hydroxyl ion formation increased the preference for Fe deposition in the electrolyte above that for Co. When 1 g/L saccharin was added to the electrolyte, the Fe content decreased to 31.8 wt%, and the Co content increased to 68.2 wt%. The composition of the metals remained steady at higher saccharin

contents. These results indicate that the presence of saccharin in the electrolyte system is beneficial to reducing the deposition of the less noble metal (Fe) from the electrolyte system.



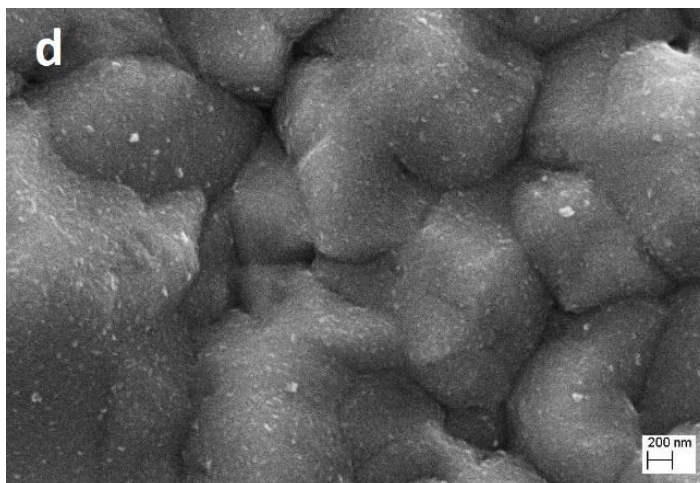
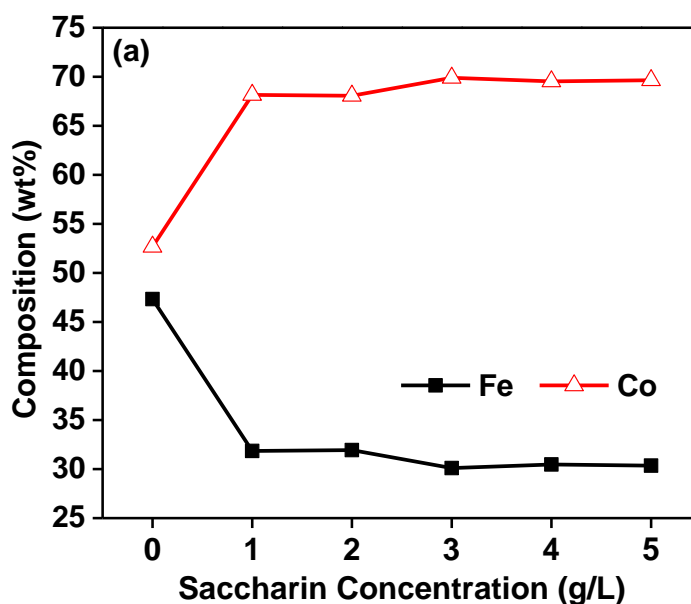


Figure 3. SEM micrographs of the FeCo films electrodeposited from an electrolyte without saccharin at room temperature (a) and from an electrolyte containing 1 g/L of saccharin at different deposition temperatures, namely, room temperature (b), 5 °C (c) and 50 °C (d).

The ratio of the metal content in the deposits to the metal content in the electrolytes calculated by Equation 1 confirmed the effect of saccharin on the anomalous co-deposition, which is one of the challenges in the electrodeposition of iron-group metals. Fig. 4b shows the composition ratio evaluated from FeCo films electrodeposited from electrolytes with different saccharin concentrations. Without saccharin, the composition ratio of Fe was 2.47, which then decreased significantly to 1.66 with the addition of 1 g/L saccharin.



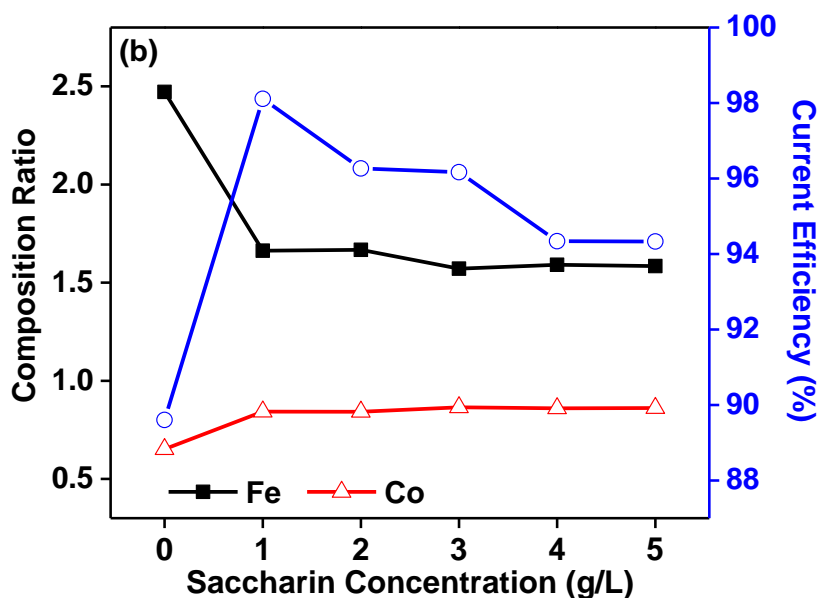


Figure 4. The elemental composition (a) and the composition ratio and current efficiency (b) of the FeCo films electrodeposited at room temperature from electrolytes containing different saccharin concentrations.

The composition ratio appeared to be steady at higher saccharin concentrations. Conversely, the Co composition ratio in the presence of 1 g/L saccharin was 0.84, which is higher than the value of 0.65 in the electrolytes without saccharin. The reduced anomalous co-deposition characteristics of Fe and Co in the electrolyte containing saccharin can be related to the reduction of the hydrogen evolution reaction and the occurrence of different complex formations in the system. First, reduction of hydrogen evolution reaction due to the adsorption of saccharin on the surface of the substrate reduced the number of hydroxyl ions forming monohydroxide ions with Fe. Second, formation of saccharin compounds occurred because of the ability of saccharinate anions to act as ligands capable of binding to Fe ions to form complexes $[\text{Fe}(\text{C}_7\text{H}_4\text{NO}_3\text{S})_2(\text{H}_2\text{O})_4]$ [37]. Different from the complex containing monohydroxide ions, this complex is a large neutral molecule that can inhibit diffusion towards the surface of the substrate.

Fig. 4b also shows that the addition of saccharin plays a significant role in increasing the current efficiency of Fe and Co co-deposition. By adding 1 g/L saccharin to the electrolyte solution, the current efficiency value increased to 98.1% in comparison with that in the absence of saccharin (89.6%). In this case, the contributing factor is the adsorption of part of the saccharinate anion on the substrate surface due to the negative delocalisation of the charge in the N-C-O bond in the molecular structure of saccharin [38]. In addition to its ability to inhibit hydrogen evolution, which has implications for increasing the efficiency of reaction currents in the system, saccharin, which binds to the surface, can also form complexes. In contrast to the complex formation in the electrolytes, the formation of ion-metal complexes with the saccharinate ions that were previously adsorbed on the substrate can reduce the number of reaction stages at the interface of the electrolyte and the substrate [39], thus accelerating the deposition process. This assumption was confirmed by the relatively high deposition rate in the presence of saccharin, as shown in Fig. 5.

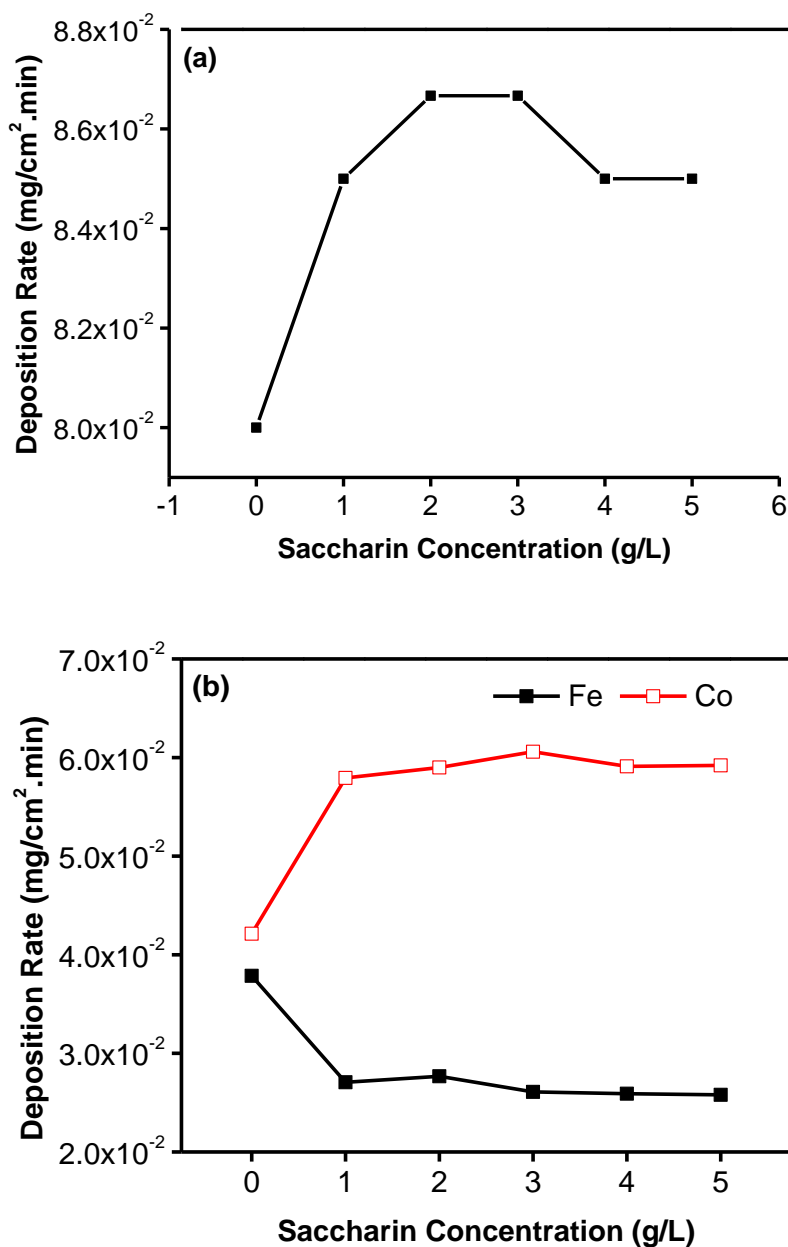


Figure 5. Total deposition rate of FeCo (a), deposition rate of Fe and Co alone (b) from the nanocrystalline FeCo electrodeposition carried out at room temperature from the electrolytes containing different saccharin concentrations from 0 to 5 g/L.

To understand the effect of deposition temperature, in addition to the room temperature previously applied, electrodeposition of the FeCo films was also conducted at a lower temperature (5 °C) and a higher temperature (50 °C). As shown in Fig. 6, different temperatures resulted in different atomic compositions of Fe and Co. The Co content increased with increasing electrodeposition temperature, whereas the Fe content decreased. At a deposition temperature of 5 °C, the contents of Fe and Co were 32.74 wt% and 67.26 wt%, respectively. At a deposition temperature of 50 °C, the contents

of Fe and Co were 29.50 wt% and 70.59 wt%, respectively. These deposit compositions changed the composition ratios for both Fe and Co (Fig. 6b).

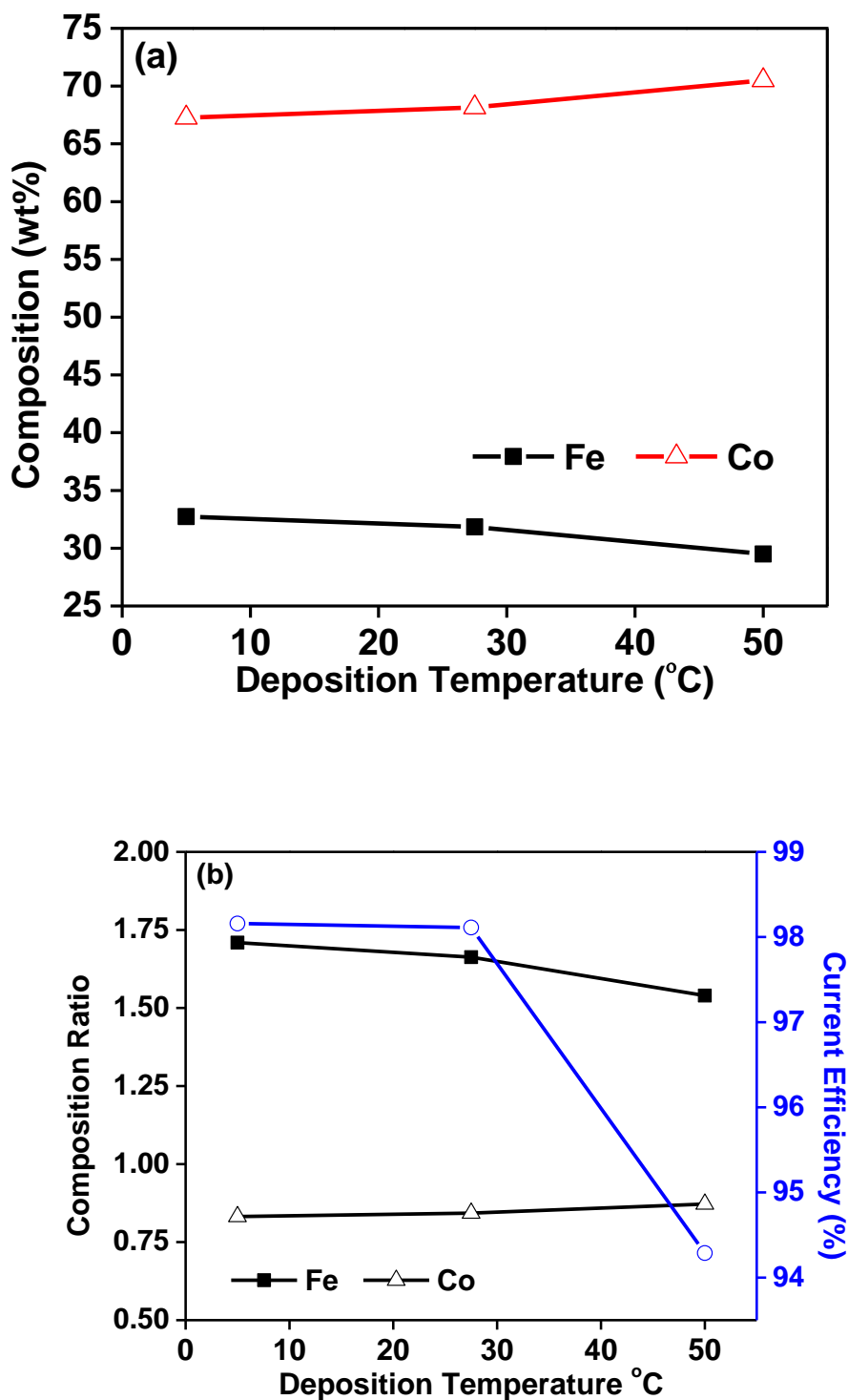
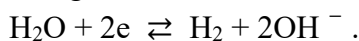


Figure 6. Fe and Co composition (a) and composition ratio and current efficiency (b) of nanocrystalline FeCo electrodeposited from electrolytes containing 1 g/L saccharin at different deposition temperatures of 5 °C to 50 °C.

In this case, the composition ratio for Fe decreased slightly at high temperatures from 1.70 (5 °C) to 1.53 (50 °C), whereas that of Co slightly increased from 0.83 at 5 °C to 0.87 at 50 °C. These results indicate an increase in the deposition preference for more noble metal (Co) at higher temperatures as a consequence of the increased desorption of the ion species (Fe^+_{ads} and $\text{Fe}(\text{OH})^+_{\text{ads}}$) from above the surface of the substrate [40], which led to a decrease in the Fe deposition rate. In addition, at high temperatures, the noble metal deposition preference increased, and this preference was affected by the cathode potential that changed as the temperature changed. At high temperatures, the cathode potential became more positive. This condition made Co deposition easier than Fe deposition, as Co had a more positive reduction potential than Fe. Conversely, at low temperatures (5 °C), the cathode potential became more negative, and thus, the deposition of Fe increased. These results are consistent with the basic characteristics of metal deposition, in which metals more noble than Fe group metals increase at higher deposition temperatures [41].

As shown in Fig. 6b, temperature also affected the current efficiency of the FeCo electrodeposition. At 5 °C, the current efficiency was recorded to be 98.2%, and it decreased to 94.3% when the temperature increased to 50 °C. This change is associated with the increase in hydrogen partial flow, which increases the formation of hydrogen gas at a high deposition temperature [42] according to the following reaction:



This condition reduced the reduction of metal ions and thus reduced the deposition efficiency. The high hydrogen partial flow can also increase the pH of the solution, thus causing the metal to be more easily hydrolysed and the formation of metal hydroxide compounds at the interface of the bulk electrolyte with electrodes. This condition can impede the reduction mechanism of metal ions and monohydroxide ions. Although deposition should take place faster at high temperatures because it can occur at lower potentials, this process seems to be disrupted by the formation of metal salts (metal hydroxide) [43].

4. CONCLUSION

In summary, the nanocrystalline FeCo film was successfully electrodeposited on a flexible ITO-PET substrate. The addition of saccharin was found to be beneficial in reducing anomalous co-deposition through the formation of a saccharin complex with Fe ions as a large neutral species that can inhibit diffusion towards the surface of the substrate. Anomalous co-deposition characteristics were also decreased at high temperatures, although the changes were not as significant as those observed by adding saccharin additives. The effect of deposition temperature is related to the cathode potential, which becomes more positive at high temperatures and makes the more noble metal (Co) easier to deposit than the less noble metal (Fe). The current efficiency increased with the addition of saccharin. The adsorption of saccharin molecules on the electrode surface is believed to inhibit the hydrogen evolution reaction, which has a positive effect on the use of current for metal reduction in the system. In addition, saccharin molecules adsorbed on the surface can help to bind metal ions so that they can reduce the number of reaction stages. Conversely, the increase in deposition temperature caused a decrease in the current

efficiency that was attributed to the partial current of hydrogen, which increases with the increase in deposition temperature, thereby suppressing metal reduction. A high-temperature system can also increase the formation of metal hydroxide compounds as a result of an increase in the pH of the solution. The successfully electrodeposited film was the nanocrystalline phase of FeCo with a very fine crystallite size. The saccharin additive and the electrodeposition temperature were also found to affect the morphology and crystallite size of FeCo. The role of saccharin and the deposition temperature in modifying the microstructure of the film should be an interesting topic for further investigation.

ACKNOWLEDGEMENT

The authors would like to thank Universitas Negeri Jakarta and the Ministry of Research, Technology and Higher Education of the Republic of Indonesia for the financial support under the research scheme Penelitian Terapan with contract no. 27/SP2H/DRPM/LPPM-UNJ/III/2019.

References

1. W. Sides, N. Kassouf, Q. Huang, *J. Electrochem. Soc.*, 166 (2019) D77–D85.
2. W. Lu, P. Huang, C. He, B. Yan, *Int. J. Electrochem. Sci.*, 7 (2012) 12262–12269.
3. N. V. Myung, D.Y. Park, D.E. Urgiles, T. George, *Electrochim. Acta*, 49 (2004) 4397–4404.
4. W. Lu, M. Jia, M. Ling, Y. Xu, J. Shi, X. Fang, Y. Song, X. Li, *J. Alloys Compd.*, 637 (2015) 552–556.
5. B.Y. Zong, Y.P. Wu, P. Ho, W.L. Chan, Y. Yang, C. Zhao, T.W. Deng, N.N. Phuoc, Z.W. Li, *J. Alloys Compd.*, 730 (2018) 284–290.
6. C. Qiang, J. Xu, S. Xiao, Y. Jiao, Z. Zhang, Y. Liu, L. Tian, Z. Zhou, *Appl. Surf. Sci.*, 257 (2010) 1371–1376.
7. D. Cao, H. Li, Z. Wang, J. Wei, J. Wang, Q. Liu, *Thin Solid Films*, 597 (2015) 1–6.
8. Y. Zhang, D.G. Ivey, *Mater. Chem. Phys.*, 204 (2018) 171–178.
9. T. Chotibhawaris, T. Luangvaranunt, P. Jantaratana, Y. Boonyongmaneerat, *Intermetallics*, 93 (2018) 323–328.
10. L.U. Ricq, F. Lallemand, M.P. Gigandet, J. Pagetti, *Surf. Coat. Technol.*, 138 (2001) 278–283.
11. F. Lallemand, L. Ricq, M. Wery, P. Berçot, J. Pagetti, *Surf. Coatings Technol.*, 179 (2004) 314–323.
12. W. Lu, P. Huang, C. He, B. Yan, *Int. J. Electrochem. Sci.*, 8 (2013) 914–923.
13. D. Kim, D. Park, B.Y. Yoo, P.T.A. Sumodjo, N. V Myung, *Electrochim. Acta*, 48 (2003) 819–830.
14. S.H. Teh, I.I. Yaacob, *IEEE Trans. Magn.*, 47 (2011) 4398–4401.
15. N.M. Nik Rozlin, A.M. Alfantazi, *Mater. Sci. Eng. A*, 550 (2012) 388–394.
16. B. Crozier, Q. Liu, D.G. Ivey, *J. Mater. Sci. Mater. Electron.*, 22 (2011) 614–625.
17. J.J. Alcaraz-Espinoza, H.P. de Oliveira, *Electrochim. Acta*, 274 (2018) 200–207.
18. S. Budi, B. Kurniawan, D.M. Mott, S. Maenosono, A.A. Umar, A. Manaf, *Thin Solid Films*, 642 (2017) 51–57.
19. J. Yu, F. Xie, Z. Wu, T. Huang, J. Wu, D. Yan, C. Huang, L. Li, *Electrochim. Acta*, 259 (2018) 968–974.
20. I. Tabakovic, S. Riemer, N. Jayaraju, V. Venkatasamy, J. Gong, *Electrochim. Acta*, 58 (2011) 25–32.
21. N. V Myung, K. Nobe, *J. Electrochem. Soc.*, 148 (2001) 136–144.
22. S. Riemer, J. Gong, M. Sun, I. Tabakovic, *J. Electrochem. Soc.*, 156 (2009) 439–447.
23. A. Chansena, S. Sutthiruangwong, *J. Magn. Magn. Mater.*, 429 (2017) 251–256.

24. F. Lallemand, L. Ricq, M. Wery, P. Berçot, J. Pagetti, *Appl. Surf. Sci.*, 228 (2004) 326–333.
25. W. Lu, P. Huang, K. Li, P. Yan, Y. Wang, B. Yan, *Int. J. Electrochem. Sci.*, 8 (2013) 2354–2364.
26. C. Nie, L. Pan, H. Li, T. Chen, T. Lu, Z. Sun, *J. Electroanal. Chem.*, 666 (2012) 85–88.
27. L. Jinlong, L. Tongxiang, W. Chen, *J. Solid State Chem.*, 240 (2016) 109–114.
28. A.M. Rashidi, A. Amadeh, *Surf. Coat. Technol.*, 204 (2009) 353–358.
29. J.C.. Smith, R.S.; Godycki, L.E.; Lyod, *J. Electrochem. Soc.*, 108 (1961) 996–998.
30. W. Lu, P. Huang, K. Li, P. Yan, Y. Wang, B. Yan, *Int. J. Electrochem. Sci.*, 8 (2013) 2354–2364.
31. M. Waldiya, D. Bhagat, I. Mukhopadhyay, *J. Electroanal. Chem.*, 814 (2018) 59–65.
32. H.R. Sadig, L. Cheng, T. fei Xiang, *Arab. J. Chem.*, 12 (2019) 610–620.
33. N. Aboudzadeh, C. Dehghanian, M.A. Shokrgozar, *Surf. Coatings Technol.*, 375 (2019) 341–351.
34. C. Srivastava, S.K. Ghosh, S. Rajak, A.K. Sahu, R. Tewari, V. Kain, G.K. Dey, *Surf. Coatings Technol.*, 313 (2017) 8–16.
35. Y. Yang, *Int. J. Electrochem. Sci.*, 10 (2015) 5164–5175.
36. M. Matlosz, *J. Electrochem. Soc.*, 140 (1993) 2272–2279.
37. F. Lallemand, L. Ricq, E. Deschaseaux, L. De Vettor, P. Berçot, *Surf. Coatings Technol.*, 197 (2005) 10–17.
38. S.M.H.Z. Shirazi, M.E. Bahrololoom, M.H. Shariat, *Surf. Eng. Appl. Electrochem.*, 52 (2016) 434–442.
39. L. Altamirano-Garcia, J. Vazquez-Arenas, M. Pritzker, R. Luna-Sánchez, R. Cabrera-Sierra, *J. Solid State Electrochem.*, 19 (2014) 423–433.
40. T. Lee, L. Chang, C. Chen, *Surf. Coat. Technol.*, 207 (2012) 523–528.
41. G.P. Pavithra, A.C. Hegde, *Appl. Surf. Sci.*, 258 (2012) 6884–6890.
42. X. Qiao, H. Li, W. Zhao, D. Li, *Electrochim. Acta*, 89 (2013) 771–777.
43. R.E.N. Xiu-lian, W.E.I. Qi-feng, L.I.U. Zhe, L.I.U. Jun, *Trans. Nonferrous Met. Soc. China*, 22 (2012) 467–475.